Optimization based planning of urban energy systems: Retrofitting a Chinese industrial park as a case-study

Xuyue Zheng[a], Yuwei Qiu[a], Xiangyan Zhan[a], Xingyi Zhu[a], James Keirstead[b], Nilay Shah[c],

Yingru Zhao[a],*

[a] *School of Energy Research, Xiamen University, Xiamen 361005, China*

[b] *Department of Civil and Environmental Engineering, Imperial College London, London SW7 2AZ, UK*

[c] *Department of Chemical Engineering, Imperial College London, London SW7 2AZ, UK*

Abstract

Optimization modelling is popular method for evaluating the design of energy systems in a given urban area. This is largely because the design of urban energy systems requires one to make complex decisions about the choice of technologies, their location, and the fuels they use. This study presents an approach for modelling and optimizing decisions for retrofitting urban energy systems, with a focus on the optimal configuration and operation of supply side and demand side technologies required to satisfy the energy requirements. A MINLP model is formulated in GAMS and solved using Lindo optimizer. A case study in urban China is presented to verify the model and to identify opportunities for systems integration. Three scenarios are analysed, namely baseline, high energy price and low carbon, and the results show that a potential reduction in space heating and CO_2 emissions of up to 57.7% and 50% are possible by retrofitting building envelopes with PV, GSHP and natural gas CHP systems. Sensitivity analysis and multi-objection optimization further indicate that CO_2 emission plays the most important role in decision-making. This approach enables us to identify design trade-offs of complex urban energy systems so as to evaluate the potential of alternative technology mix.

Keywords: Urban energy systems; Retrofit; Optimization model; Supply side and demand side; Configuration and operation.

* Corresponding author. Tel.: +86 592 5952781; Fax: +86 592 2188053.

E-mail address: yrzhao@xmu.edu.cn (Y. Zhao).

1. Introduction

Cities are increasingly reaching the top of the agendas of various initiatives worldwide aimed at reducing the cost and carbon footprint of energy products, services and activities [1, 2]. As cities are home to over 50% of the world's population and that percentage is predicted to increase to 70% by 2050 [3, 4], it is crucial to make cities more energy efficient and environmentally friendly in a cost-effective manner. The key to coordinating urbanization with the utilization of energy resources lies in the rational planning of urban energy resources and the configuration optimization of urban energy systems, based on which a comprehensive evaluation from the perspectives of environmental sustainability, energy conservation and economics can be achieved, and hence the feasible solutions of an urban energy system and its future development can be proposed [5-7].

Optimization models play a powerful role in helping assist decision makers with plans for designing and retrofitting energy systems. With state-of-the-art optimization algorithms, local governments and property developers are able to find the best solutions for technology upgrades of existing energy systems. In fact, decades of progress have been made on optimization modelling for strategic decisions on the planning and retrofits of urban energy systems. Back in the 1990s, Gustafsson et al. [8] already used optimization techniques for planning urban retrofits, in which study MILP models have been formulated with an objective function to minimize the installation and operation costs for a range of retrofit strategies of multi-family buildings in Sweden. Adamo et al. [9] proposed a static model to optimize district

heating networks, with a cost function and iterative procedure being used to determine the minimum value corresponding to the optimal pipe size and insulation thickness. Henning provided a dynamic liner programming (LP) model MODEST to minimize the capital and operation costs of energy supply and demand side management[10].

In recent years, increasing efforts have been made towards optimizing energy systems at urban or technological scale [11-13]. In terms of urban-scale modeling and case studies, Jennings et al. developed an optimization model for retrofitting the residential energy systems of an urban area of 29.6 km^2 in London [14]. Rolfsman et al. investigated the municipal energy system of an area of 42 km^2 [15]. Giannoulis et al. evaluated a distributed generation in an isolated grid on Lesvos island, which covers an area of 1632 km^2 [16]. While the areas under discussion in the three studies summarized above have varied in size, the modeling and optimization results are equally rigorous.

On the other hand, considerable progress has been made on technological scale optimization of urban energy systems. For example, Capuder et al. [17] introduced an unified and synthetic optimization model to evaluate the techno-economic and environmental characteristics of various distributed multi-generation options. Dong et al. [18] proposed a bi-level programming model for the planning of distributed energy supply networks. Bridier et al. [19] provided an optimal design of storage system coupled with intermittent renewable energies. Hong et al. [20] presented a framework for establishing the optimal implementation

strategy of a fuel cell-based CHP system for multi-family housing complex. Bakken et al. [21] proposed a hierarchical approach for the superstructure-free synthesis and optimization of energy supply systems.

The idea of adaptable, integrated and networked urban energy systems holds opportunities and challenges for both China and other countries in the world [22, 23]. To date, methods of calculating the best allocation of urban energy resources with models that describe urban energy systems have formed the subject of many previous publications [24, 25]. However, as an interdisciplinary subject, this kind of research is only in its infancy with many problems and challenges still remaining. First of all, urban energy systems is a complex system engineering subject, which comprises a series of processes including the production, transportation, storage, conversion and distribution of energy, with an ultimate object of satisfying the energy demand of end-users. The quantity, flow direction, and condition change of various energy flows in the system, as well as the performance characteristics and operation conditions of different facilities all have impact on the final energy supply. In many cases these sectors are treated as separate by decision makers, while there are closer interactions that need to be addressed, with clear potential for techno-economic and environmental optimization from both operational and planning perspectives. Secondly, although abundant studies have been published on describing and optimizing urban energy systems, no explicit discussions can be found regarding the influence of building envelope retrofit on the optimal operation strategy of the entire system.

More importantly, there are a limited number of optimization-based approaches applied to urban development in China. The reason for the historical lack of interest is argued as due to both lack of practical data and insufficient computing capability.

In this context, a newly developed MINLP (mixed integer nonlinear program) modeling framework is formulated in the present study to determine whether or not modern optimizers have the capacity for dealing with resource planning and system retrofitting problems in urban China. The approach used here improves on existing urban energy system models in different ways. First, the model incorporates both supply side and demand side technologies, with an objective to minimize the total cost while meeting the heating and electricity demand of buildings. Second, the model has ability to generate and analyze a large number of scenarios. Third, it can analyze a number of models while varying one or a few key parameters to explore the solution space. The results of this optimization are described by three scenarios for the test case based on real-life data, with sensitivity analysis and multi-objective evaluations. A mix of technologies that will best meet the energy service requirements during the period of 2014-2025 is defined. Note that the year of 2014 when nothing has been changed, is taken as the reference case for comparison.

2. Model description

Urban energy systems comprise both supply side and demand side technologies, by which

thermal energy and electricity are produced, converted and consumed in a given urban area. The number of alternative arrangements of technologies introduces many degrees of freedom, particularly where large numbers of buildings and networks are in play. The problem being modeled in the present study is to determine the best combination of new and existing technologies to meet the energy demand of buildings subject to practical constraints. The technologies considered include both new and traditional powered technologies, as well as centralized and distributed technologies.

A comprehensive and integrated model is built upon the practical energy requirement of a 7 km^2 industrial park located in Xi'an, China. This industrial park is managed by the ShaanGu Power Company Ltd. Historically they manufacture machinery, but more recently they have expanded into utility service provision, managing the energy for the redevelopment of their factory. The industrial park under study can be disaggregated into two building clusters, i.e., an industrial area and a residential area, as shown in Fig. 1. According to the observations, the electricity demand of these buildings has been increasing steadily in recent years. The existing power supply facilities for these buildings, e.g., conventional coal-fired boilers and incumbent electric heaters etc., have been used for decades and became quite inefficient or even not operational, and hence will not be able to satisfy the future energy demand. Therefore, one of the major purposes of this retrofit is to use cogeneration and efficient decentralized heating and cooling technologies to replace the old age supply side energy facilities. Distributed energy

technologies such as natural gas CHP plant, high efficiency condensing gas boilers, GSHP (ground source heat pump), photovoltaic panel, etc., have been considered as alternative supply side technologies as they are thought suitably representative of the generic commercial alternatives currently available in China.

On the demand side, it is known that for residential and industrial buildings, approximately 50% of energy loss is due to heat transfer out of the building envelope. Nevertheless, heat loss from walls and windows can be significantly reduced by means of thermal insulation[26]. Therefore, the thermal insulation of building envelopes is another focus of the present research. A range of thermal insulation measures have been considered as well as demand side technologies in this study, including window glazing, wall insulation, floor insulation, roof insulation and door insulation.

A MINLP (mixed-integer nonlinear programming) model is therefore formulated in GAMS (Rev 240 WEX –VS8 24.0.2 x86) using the Lindo optimizer (version 7.0.1.497) to seek for the optimal arrangement of aforementioned technologies. The computer used to solve the problems has 8GB of RAM and 64-bit Intel Core i5 processor, with Windows 10 operating system. The objective function of the model is to minimize costs, whose main decision variables refer to the type, size and operating strategy of the technologies, which will be described in Section 2.1. Unlike previous studies where the real time variations of energy demand were normally ignored, the effect of demand fluctuation is considered in the present model.

This model will help to address the following question: Given an urban area, with its available renewable resources, buildings and their related consumption profiles, which combination of energy conversion technologies will be best suited to meet the local energy services, and how will these technologies be integrated and operated?

2.1 Demand side

In the present model, heating demand refers to both residential and industrial building space heating requirements. Cooling demand is considered as part of the electricity demand instead of being calculated separately as cooling can be provided by means of mechanical ventilation or electric air-conditioning. The amount of space heating required primarily depends on replacing lost heat to meet a desired temperature level [14]. According to the Chartered Institution of Building Services Engineers[27], building heat loss can be calculated as the sum of all the elements' heat loss of the entire building envelope. The building envelope consists of all the building elements that separate the inside from the outside, including exterior wall, exterior windows, roof, floor and exterior door, etc.

Accordingly, the temperature difference between the external environment and the internal temperature of the building is used to calculate its heat loss:

$$Q_{i,y,s,h} = \sum_{e} A_{i,y,e} \cdot U_{i,y,e} \cdot (T^{in} - T^{out}_{s,h}) \quad (1)$$

where the subscripts *y*, *s* and *h* represent the temporal sets of years, seasons and hours

respectively, A and U denote the surface area of a building element e and its corresponding thermal conductivity, T^{out} is the external environmental temperature that is indexed by season s and hourly period h, T^{in} is the designed indoor temperature which is given as constant (18℃) [28], Q represents the sum of building heat loss for each spatial area i in the hourly period h, and is equal to the heat supplied by heating systems as described in Section 3.2. Note that 24 hours for a day are divided into six time periods on average, i.e., h_1 to h_6. Considering that the local population growth will lead to an increasing area of building stocks, the surface area of each building element is calculated as a function of its growth rate:

$$A_{i,y,e} = A_{i,y-1,e} \cdot (GR_{i,y} + 1) \tag{2}$$

The surface areas and corresponding thermal conductivities for different building elements of the case study can be found in Table 1 and Table 2. Note that the values of thermal conductivity after retrofit are chosen according to the National Energy Saving Standards in China.

Based on real-world weather data of the test case, the average daily temperature throughout the whole year is plotted in Fig. 2, where the outdoor temperature T^{out} in winter is shown to be varied roughly between -5℃ to 5℃. It should be noted that the data in Fig. 2 is the average temperature of each time period h.

Reducing the thermal conductivity U of a building envelope may decrease its existing heat loss, which in turn will lead to a reduction of heating requirement. A thermal conductivity balance relates the value in the previous time period to the current time period is given as

follows:

$$U_{i,y,e} = U_{i,y-1,e} + \sum_{ds} \frac{RA_{i,ds,y,e}}{A_{i,e}} \cdot IU_{i,ds,e} \tag{3}$$

where *RA* is introduced as a decision variable to represent the area that is retrofitted of each building envelope for spatial area *i* in time period *y*. *IU* is defined as the impact of a thermal insulation measure *ds* on the building element *e* in spatial area *i*, whose value should be negative.

2.2. Supply side

A network flow model is developed in the present study to effectively illustrate the energy flow of the urban energy system under study, as depicted in Fig. 3, where the electricity grid and heating network are integrated via the connection of various energy conversion units to supply electricity and heating to the end-users, i.e., buildings. Note that the supplementary heating devices refer to the existing indoor heating devices, for instance electric radiators which are utilized only to cover the peak heat demand or just for backup usage.

The energy balances of the present model are formulated in Eqs. (4)-(7), representing constraints on its energy flows：

$$X_{1,s,h} + X_{2,s,h} = X_{3,s,h} + X_{4,s,h} + X_{7,s,h} \tag{4}$$

$$X_{3,s,h} + X_{5,s,h} = X_{6,s,h} \tag{5}$$

$$X_{8,s,h} + X_{9,s,h} + X_{10,s,h} + X_{12,s,h} = X_{11,s,h} + X_{14,s,h} \tag{6}$$

$$TS_{s,h} = TS_{s,h-1} + X_{11,s,h} - X_{12,s,h} - X_{13,s,h} \quad (7)$$

where variables X are energy flows to and from different units. $X_{14,s,h}$ represents the sum of the thermal output energy from the supply side technologies, which should be equal to the heating requirement of demand side buildings. $TS_{s,h}$ and $TS_{s,h-1}$ represent the storage of thermal energy in current and previous hourly time periods, respectively. $X_{11,s,h}$ and $X_{12,s,h}$ denote the thermal energy being stored or consumed in time period h, respectively. $X_{13,s,h}$ represents the storage losses, the calculation of which, as indicated in Ref. [29], is based on the definition of an hourly heat loss coefficient.

Note that the electricity imported from and exported to the grid, i.e., X_5 and X_4, cannot occur simultaneously:

$$X_{4,s,h} \cdot X_{5,s,h} = 0 \quad (8)$$

This is to avoid an unreasonable situation that when the electricity price is off-peak, all the electricity required by the demand side buildings will be imported from the grid, while all the power generated by the supply side technologies will be sold to the grid.

The above constraints ensure that the flow of energy coming into a unit is equal to the demand plus the flow leaving the unit.

2.3. Technology constraints

This section will discuss the optimal combination of existing and new technologies in

different time periods. New technologies that can be selected to replace the existing inefficient technologies include natural gas CHP (combined heat and power), high-performance condensing boiler, GSHP (ground source heat pump), gas boiler, solar PV, and thermal storage equipment. All the technologies considered are defined as set *ss*, which include both existing and new technologies. The new technology set is specifically defined as *ss`* which is apparently part of the set *ss*.

Regarding new technologies, there are two of them being modelled in the present study, i.e., solar PV and GSHP. The electricity generated by PV is limited mainly by two constraints, namely, the solar irradiance δ_{pv} and the number of PV panels in year *y* $NST_{pv,y}$, as given in Eq. (9):

$$X_{1,s,h} = \sum_{i} \eta_{pv,s,h} \cdot \delta_{pv,s,h} \cdot NST_{i,pv,y} \cdot \varepsilon_{pv} \qquad pv \in ss' \tag{9}$$

where X_1 is the power output of PV, η_{pv} is PV efficiency which is taken as a constant equal to 14.2% [30], ε_{pv} is the average size of a PV panel, and δ_{pv} represents the solar irradiance at a specific time period whose value can be obtained from local Meteorological Bureau.

An important constraint of PV application is the available roof space $A_{i,pv}$ in spatial area *i* for PV installation:

$$NST_{i,pv,y} \cdot \varepsilon_{pv} \le A_{i,pv} \qquad pv \in ss' \tag{10}$$

Similarly, the installation of GSHP is also limited by the available space:

$$NST_{i,gshp,y} \cdot \varepsilon_{gshp} \le A_{i,gshp} \qquad \text{gshp} \in ss' \tag{11}$$

where $NST_{gshp,y}$ represents the number of GSHPs in year y, ε_{gshp} the average area required per GSHP installation, and $A_{i,gshp}$ the available area for GSHP installation in spatial area i.

Other constraints for GSHP are given as follows:

$$COP_{s,h} = 0.00073\Delta T_{s,h}^2 - 0.15\Delta T_{s,h} + 8.77 \tag{12}$$

$$EC_{i,gshp,s,h} = OE_{i,gshp,s,h} \cdot COP_{s,h}^{-1} \tag{13}$$

$$\sum_i EC_{i,gshp,s,h} \cdot NST_{i,gshp,y} = X_7 \tag{14}$$

$$\sum_i OE_{i,gshp,s,h} \cdot NST_{i,gshp,y} = X_{10} \tag{15}$$

where $\Delta T_{s,h}$ represents the time-varied temperature difference between soil and GSHP outlet. COP is the coefficient of performance for GSHP, the calculation of which is according to an empirical relationship [31] described by Eq. (12). EC_{gshp} and OE_{gshp} represent the energy input and output of a single GSHP, respectively.

The non-renewable technologies include natural gas CHPs and boilers. Boilers refer to both non-condensing boilers and condensing boilers. CHPs supply both electricity and heating, while boilers provide only heating to the demand side buildings. The number of existing and new technologies of supply side NST as well as the total building heating load Q are constrained by the following relationship:

$$\sum_i \sum_{ss} NST_{i,ss,y,s,h} \cdot CAP_{ss} \geq \sum_i Q_{i,y,s,h} \cdot \alpha \tag{16}$$

where CAP represents the design capacity of a supply side heating equipment, Q is defined as the heating load of buildings at a specific time period, and α is the design margin which is

suggested as 20% above the heating load at design conditions to allow for intermittent heating [14].

To balance the number of supply side equipments in year *y* and the number of existing equipments in the previous year *y-1*, Eq. (17) is given:

$$NST_{i,ss,y} = NST_{i,ss,y-1} + \sum_{ss'} SI_{i,ss',y} \cdot RT_{i,ss',ss} \qquad ss' \in ss \tag{17}$$

where *SI* is an integer variable which is defined as the number of newly invested or retrofitted equipments, *RT* is defined as the equipment replacement parameter to reflect the effect of multiple exchanges of equipment, whose value is either -1or1.

In terms of output, the electricity and thermal energy generated by CHPs and boilers are calculated as follows:

$$\eta_{chp}^{el} \cdot X_{15,s,h} = X_{2,s,h} \tag{18}$$

$$\eta_{chp}^{th} \cdot X_{15,s,h} = X_{8,s,h} \tag{19}$$

$$\eta_{boiler}^{th} \cdot X_{16,s,h} = X_{9,s,h} \tag{20}$$

where η^{el} and η^{th} represent the electrical efficiency and thermal efficiency, respectively. X_{15} and X_{16} represent the amount of energy carried in the fuel flows that to be consumed by the supply side equipments. Other constraints about the existing technologies are given as follows:

$$\sum_i NST_{i,chp,s,h} \cdot CAP_{chp,s,h} = X_{8,s,h} \tag{21}$$

$$\sum_i NST_{i,boiler,s,h} \cdot CAP_{boiler,s,h} = X_{9,s,h} \tag{22}$$

$$\sum_i NST_{i,gshp,s,h} \cdot CAP_{gshp,s,h} = X_{10,s,h} \tag{23}$$

$$CAP_{ss,s,h}^{\min} \cdot \mu_{ss,s,h}^{\min} \le CAP_{ss,s,h} \le CAP_{ss,s,h}^{\max} \cdot \mu_{ss,s,h}^{\max} \quad (24)$$

where CAP is the operating capacity of technologies ss at time period h, $CAP^{\min}$ and CAP^{max} are defined as the minimum and maximum designed capacity of technologies ss. Considering in practice the demand of energy may be intermittent and technologies are allowed to be operated at part load conditions, a load factor μ is introduced as an on-off coefficient to determine the effect of minimum/maximum load of CHPs. According to previous research, a 25%-100% part load factor is selected to represent the switch on or off of CHPs [32], as indicated in Table 3, while for other technologies the part load factor can be varied between 0 and 100%.

2.4. CO_2 emission

Carbon dioxide emissions of the urban energy system are mainly due to its natural gas consumption and electricity imported from the grid. Therefore, the CO_2 emissions are calculated as sum of these direct and indirect emissions：

$$EM_y = \sum_s \sum_h X_{15,y,s,h} \cdot \gamma_{gas} + \sum_s \sum_h X_{16,y,s,h} \cdot \gamma_{gas} + \sum_s \sum_h X_{5,y,s,h} \cdot \gamma_{el} \quad (25)$$

where EM_y represents the total CO_2 emissions in year y, γ_{gas} represents the CO_2 emissions per unit consumption of gas, and γ_{el} denotes the CO_2 emissions per unit generation of grid electricity.

2.5. Objective function and cost functions

The overall objective of the present model is to minimize the total costs of the urban energy system over a time horizon to satisfy the fluctuant energy demand. Costs are due to both maintaining and operating technologies (operating costs) as well as the investment in new and retrofit technologies (capital costs).

The objective function can be expressed as the sum of capital costs *CC* and operating costs *OM*, and minus the income *IN* obtained by selling extra electricity to the grid:

$$\min \sum_{y} \frac{1}{(1+r)^{y}} \cdot (CC_{y} + OM_{y} - IN_{y}) \tag{26}$$

where *r* denotes the discount rate, which is to discount all future costs and benefits to their today's value, i.e., net present value (NPV). Note that NPV is identified as the economic criterion best suited for single-objective flowsheet optimization.

The capital costs are composed of two parts: i) the investments *RA* in demand side to retrofit building envelopes, and ii) the investments *SI* in supply side to cover the costs of machinery or equipment, as shown in Eq. (27):

$$CC_{y} = \sum_{i} \sum_{ds} \sum_{e} RA_{i,ds,e,y} \cdot DSP_{ds,e} + \sum_{ss} SI_{ss,y} \cdot SSP_{ss} \tag{27}$$

where $DSP_{ds,e}$ is the retrofitting cost per unit area of the demand side building element *e*, and SSP_{ss} represents the cost of the supply side equipment which is defined by the set *ss*.

The operating and maintenance costs can be divided into three parts: i) costs of maintaining equipments, ii) costs of operating equipments for instance fuel consumption, and iii) costs of electricity bought from the grid:

$$OM_y = \sum_i \sum_{ss} NST_{i,ss,y} \cdot SM_{ss} + \sum_s \sum_h X_{17,y,s,h} \cdot GP + \sum_s \sum_h X_{5,y,s,h} \cdot SE_h \quad (28)$$

where SM_{ss} denotes the maintenance cost for the supply side equipment which is defined by the set *ss*, *GP* is the price of natural gas, and SE_h refers to the price of grid electricity at time *h*. It should be noted that gas price is considered as constant while a time-of-use (TOU) pricing is considered for electricity specifically.

The income obtained by selling the extra amount of electricity, i.e., X_4, to the grid is calculated as follows:

$$IN_y = \sum_s \sum_h X_{4,y,s,h} \cdot FP \quad (29)$$

where *FP* is the feed-in tariff of electricity.

3. Results and discussion

The proposed model for the urban energy system is employed for the case of the industrial park which contains approximately ten thousand residences. The model as defined is formulated in GAMS with an objective to identify the best mix and operation strategies of technologies under three optimization scenarios, namely, baseline, high energy price, and low carbon emissions. For each scenario the minimization of the overall costs is always chosen as the objective function, but various constraints may be added or modified. The overall model includes approximately 11,000 equations, 28,000 constraints and 100,000 variables. The CPU time required to solve the problem is less than one minute,

In the baseline scenario, current energy prices in China are used and there is no limit on carbon emissions. While in the scenario of high energy price, the prices of gas and electricity are assumed to be 50% or 100% higher than the baseline prices. It should be noted that gas price is considered as constant as 2.3 RMB/m^3. The 24 hours of a day is divided into several periods, i.e., valley period h_1-h_2, flat period h_4-h_5, peak period h_3 and h_6. The valley price, flat price and peak price of electricity are 0.22 RMB/kWh, 0.54 RMB/kWh and 0.86 RMB/kWh respectively, which values are provided by the local Price Control Administration. For the low carbon scenario, the reduction target of CO_2 emissions is constrained to 40% or 50% lower than current emissions. Optimization results for different scenarios are summarized in Table. 4.

3.1. Baseline scenario

The optimization results for the baseline scenario indicate that 94.9% of the electricity demand of the industrial park can be sufficiently covered by a 3MW natural gas CHP plant and 4.75Ha rooftop PVs. The PV panels will occupy 23.3% of the available rooftop space. The optimal configuration and operation of supply technologies for a typical summer or winter day are illustrated in Figs. 4a and 5a.

As shown in Fig. 4a, during daytime in summer, the power demand is relatively large when the grid electricity is more expensive, therefore power generation units are operated with a large load factor to generate as much electricity as possible in order to satisfy the demand of

buildings, whereas the excess electricity is sold back to the grid. On the other hand, the energy requirements are relatively low during the night, when PV panels cannot generate electricity, whereas most of power is supplied by the CHP. Only a small amount of electricity is imported from the grid, although the price of grid electricity is off-peak during the night. Throughout the whole year, 67.2% and 27.7% of the electricity demand are supplied by the CHP plant and PV respectively, whereas the remaining 5.1% relies on the imports of grid electricity.

Regarding heating, Table 4 indicates that 12.6 MW of capacity of the existing boilers are replaced by the CHP system and condensing boilers to provide heat, which account for 22.7% and 73.7% of the total heating requirements, respectively. The remaining incumbent boilers are used as back-up heaters to cover 3.6% of the total heating load. There is no investment in GSHPs in this scenario. The total demand of heating decreases by 16.3% compared to the original demand in 2014. This reduction is mainly due to the demand side retrofit on building envelopes. According to the results in Table 4, the rates of retrofit on window glazing, roof and doors are 22.5%, 34.1% and 15.2%, respectively. It is shown that the investment in retrofit of windows, roofs and doors is greater than the investment in retrofit on walls and floors, which is mainly because the insulation of walls is less efficient than that of other building elements under the cost constraint.

3.2. Low carbon emission scenario

In order to assess how the optimal mix and operation of technologies would change when restrictions are set on the maximum amount of CO_2 emission, the low carbon scenario is investigated under two different CO_2 reduction targets.

In the first case whereby a 40% decrease in CO_2 emission is imposed, the investment on building envelope retrofitting increases slightly compared to the baseline scenario, according to the results presented in Table 4. The increase in NPV is not significant as well. The annual heating load decreases 10.5% compared to the baseline case. The investments in new technologies such as PV and GSHPs are increased, particularly in GSHPs, which is reasonable as more efficient energy usage implies lower GHG emissions.

In the second case, the target of reducing CO_2 emissions is set to be 50% less than the emissions of the baseline scenario. In order to meet this target, more new energy powered technologies, for instance PVs and GSHPs, are implemented, which in turn results in a reduction of natural gas powered generation such as CHPs and incumbent gas boilers, as indicated in Table 4. There is a substantial increase in the investments in rooftop PVs, which is almost double that of the 40% carbon reduction scenario. Regarding the demand side, there are a large number of investments in retrofitting building envelopes, leading to a significant reduction of daily heating requirements in the winter of year 2025, as can be seen from Fig. 5c.

3.3. High energy price scenario

The energy price can vary seasonally, by the time of day, and may also exhibit sharp peak prices for very short periods of time [33]. Therefore, the present study also determines how the optimal configuration of technologies changes with the variation of energy prices.

For this scenario, the electricity and gas prices are assumed to be 50% and 100% higher than that of the baseline scenario. The first distinction seen from Table 4 is in the total costs, i.e., NPV, whose value is nearly doubled in the highest energy price case compared to the baseline scenario. In the 50% case, the rate of retrofit on building envelopes is relatively low, with a maximum rate of 52.3%. While in the case of twice energy price, most of these rates are increased significantly to more than 85%. Moreover, from Fig. 5 it is seen that when prices of energy increase, the total daily heating demand in winter will decrease by 27.1% and 64.1% respectively compared to the baseline scenario. These phenomena are expected because high energy price will incentivize investments in demand reduction measures in order to minimize operating costs. Specifically, heating provided by GSHPs in this scenario is increased substantially (22.2% versus 0 for the baseline scenario), which is the highest proportion in all scenarios, as listed in Table 4.

According to the results presented in Fig. 6, the most significant change is a significant increase in the total amount of retrofit areas of the building envelopes when the energy prices are at their highest level. Yet it should be noticed that there is no floor retrofit recommended in any of the optimal solutions except for the doubled energy price scenario, which is mainly due

to its high investment cost relative to the improvement in the heat transfer performance after retrofit. Nevertheless, reducing heating supplied by the gas-driven equipment is the priority under a high energy price scenario.

Regarding the optimal solution for electricity supply, what can be easily seen from Fig. 4 is a considerable increase of PV operation compared to other scenarios. The total size of installed PV panels is 15.2 Ha and 20.4 Ha respectively, occupying 74.5% and 100% of the available rooftop space accordingly. Due to more PV generation, there is an expected increase of electricity sold back to the grid, which in turn resulting in a low amount of imports of grid electricity, as shown in Table 4.

3.4. Sensitivity analysis and multi-objective optimization

The trade-off between CO_2 emission and primary energy consumption is an important issue to consider in the design and operation of urban energy systems. The constraints of CO_2 emissions will directly affect the design of natural gas fueled CHP system and the retrofit areas of building envelop, while the constraints of energy consumption will influence the total operation strategy as well as the NPV of system. A sensitivity analysis is conducted to better understand the interactions and trade-offs between CO_2 emission and energy consumption.

Fig.7 is plotted to investigate the percentage variations in CO_2 emission reduction (CER) and energy consumption reduction (ECR) after the retrofit with different selections of technology mix. According to Fig. 7, the investment on PV, GSHP and retrofitting of building

envelops increase with the rise of the ECR and CER. Compared to the case before retrofit, the installed area of PV panels first increases slightly from 23.04% to 27.45% of the available area when CER is increased from 30% to 40%, then increases significantly from 27.45% to 54.94% of the available area when CER is raised from 40% to 50%. This is because under the constraint of minimizing NPV, 40% of CER can already be achieved when the installed area of PV panels is less than 30% of its total available area, further reduction in CO_2 emissions require more PV panels to be installed. When CER reaches 50%, the retrofit area of building envelops increases from the original 16.65% to 44.22% of the total, while the installed area of GSHP increases from 0% to 100% of its available area with an increase of CER from 30% to 45%. It can be seen obviously from the figure that the variations in technology installations under different ECR is less significant than that under different CER. When ECR reaches 50%, the installed area of PV increases from 28.92% to 46.57% of the available area, the retrofit percentage of building envelops changes only from 20.05% to 28.66%, while the installed area of GSHP increases to 100% of its available area.

Fig. 8 illustrates the interactions between CER and ECR as well as the effect of CER and ECR on the NPV and operating cost of the system. Compared to the baseline scenario, NPV increases from 3.67% to 10.91% when CER varies from 35% to 50%, while NPV only has a slight increase from 4.46% to 6.08% with the same percentage of increase in ECR. On the other hand, the operating cost changes more significantly with CER than ECR. As shown in Fig. 8,

when CER and ECR both increase from 35% to 50%, the corresponding operating cost reduces from -9.79% and -7.23% to -56.84% and -25.81%, respectively. This suggests that the operational flexibility of ECR is worse than that of CER. ECR reduces from -7.91% to -34.65% when CER increases from 35% to 50%, while CER reduces from -3.24% to -23.76% when ECR increases the same percent from 35% to 50%. This is reasonable as the reduction of CO_2 emissions will inevitably lead to the reduction in energy consumption, and vice versa. Overall, CER seems to have greater impact than ECR on the optimization results of the system. The operation cost declines more significantly with CER than with ECR. When the reduction reaches 50%, the growth rate of NPV with CER is almost twice of the growth with ECR, showing that CER requires much more capital cost to achieve than ECR, which in turn means that CER is costly than ECR.

In addition to CO_2 emission and energy consumption, NPV and operating cost are also key factors to consider in the practical planning and running of urban energy systems. Considering multiple objectives are typically required, and these objectives are sometimes conflict with each other, analyzing only one optimal solution with mono objective function is not sufficient. Therefore, an integrated model is developed as follows in a multi-objective optimization perspective to assess the comprehensive indexes of the retrofit project under study, namely, NPV, CO_2 emission and energy consumption. As formulated in Eqs. (30)-(32), the multi-objective function includes the minimization of total cost (MOTC, i.e., Eq. (26)), the

minimization of CO_2 emissions (MOCE, Eq. (30)), as well as the minimization of energy consumption (MOEC, Eq. (31)) over a time horizon.

$$MOCE = \min \sum_{y} EM_{y} \tag{30}$$

$$MOEC = \min \sum_{y} \sum_{s} \sum_{h} (X_{17,y,s,h} + X_{5,y,s,h} / \eta^{grid}) \tag{31}$$

$$\min(Z_1 \cdot \frac{MOTC}{MOTC^{ref}} + Z_2 \cdot \frac{MOCE}{MOCE^{ref}} + Z_3 \cdot \frac{MOEC}{MOEC^{ref}}) \tag{32}$$

The optimization results of three sub-objectives and the multi-objective are presented in Table 5. The subscript *ref* denotes the reference case, i.e., the initial case before retrofit. η^{grid} represents the electrical efficiency of grid [32]. Z_1, Z_2 and Z_3 are the weight coefficients defined to compare the three sub-objectives in different dimensions. The values of Z_1, Z_2 and Z_3 are 25.41%, 39.48% and 35.11% respectively, which are determined through the calculation of entropy weight method [32]. Based on this, the values of MOTC, MOCE and MOEC in Eq.(32) can be further calculated, which are 337.14 million RMB, 266.27 kt and 4008.74 TJ, respectively, decreasing 5.93%, 49.9% and 46.66% compared to that of the reference case. According to the theory of entropy method, the greater the weight is, the greater role the index plays in the comprehensive evaluation. Consequently, the results of multi-objective optimization illustrate that CO_2 emission plays the most important role in decision-making. Furthermore, the results also suggest that the order of importance of the three comprehensive indexes for the case study should be CO_2 emissions > energy consumption > NPV.

4. Conclusions

This study aims to present an approach to solve retrofit problems for urban energy systems. A robust MINLP model is developed, which rigorously optimizes the configuration, sizing and operation of urban energy systems from both demand and supply side perspectives, accounting for the time-dependant demand profiles as well as the equipment sizing and part load operations for various technologies. The objective of the model is to minimize the overal costs, subject to a number of constraints that are indexed by technological, spatial, and temporal sets in the analysis.

The proposed methodology is successfully applied to the retrofit of a real-world industrial park in urban China. A range of scenarios have been analyzed, based on which the answer to the question of how different types of technology mix meet the local energy service requirements under different circumstances is given. The analyses have highlighted several issues that need to be noted.

First, it is shown that the prices of gas and electricity are likely to have a significant impact on which technology mix might be selected. For instance, in the scenario of highest energy prices, the optimal net present value (NPV) is doubled compared to the baseline scenario. However, the total heating requirements and CO_2 emissions can be reduced by up to 57.7% and 50%, respectively, via installing rooftop PVs and GSHPs in parallel with large scale retrofit of building envelopes, which is quite different from the results of the baseline scenario.

Secondly, condensing boilers are shown to be a very effective technology for the test case, if they are combined with the CHP plants to supply heating. GSHPs on the other hand, only play a small role when the other two heating technologies are in place, yet still remain essential except for the baseline scenario.

Thirdly, various sensitivity analyses for each scenario have shown that as far as electricity is concerned, fossil fuel technologies (natural gas CHP) remain essential for the test case, and the grid (fossil fuel based electricity) still could not be completely avoided in summer. Nonetheless, the optimized selection and operation of PVs and GSHPs do provide the greatest benefit in terms of carbon emission reduction, which also illustrates the importance of new technologies.

Finally, a sensitivity analysis for CER and ECR has been carried out, showing that there are interactions and trade-offs between CO_2 emission and energy consumption. The results illustrated that CER has greater impact than ECR on the optimization results of the system. and CER is much more costly than ECR. A multi-objective optimization has been also performed to assess the comprehensive indexes of the case study, showing that the order of importance for the three indexes should be CO_2 emissions > energy consumption > NPV.

In conclusion, the proposed method is thought applicable to a wide variety of urban energy system related problems. The employment of optimization models for improved decision making at the preliminary stages of design allows a better insight into the synergies between

different sources of energies. A weakness of the present research is that cooling demand is calculated as part of the electricity requirements. Moreover, the efficiencies of supply side technologies were assumed to be constant. Enhancement of the database of technologies and building energy demands, as well as the multi-objective optimization will be major tasks in future work. Therefore, further issues about the practical feasibility of such optimization procedures need to be validated, and a more in-depth analysis of the cost and efficiency trade-offs should be performed to improve the understanding of the interactions between different technologies and different sources of energy.

Acknowledgments

The authors are grateful to the National Natural Science Foundation of China for support under grant No. 51206137. The work is also supported by the Fundamental Research Fund for the Central Universities with grant No. 20720150111. The data for the model are provided by the ShaanGu Power Co., Ltd. The authors are especially thankful to Dr. Mark Jennings for his important contributions and constructive suggestions to the modelling work.

Nomenclature

Subscripts and superscripts

i spatial area, either industrial or residential

h hour

s season

y year

e building element

ds thermal insulation measure

ss supply side equipment

$ss`$ new technologies invested in supply side

pv photovoltaic

$gshp$ ground source heat pump

el electricity

th thermal

$boiler$ incumbent boiler or condensing boiler

gas natural gas

chp combined heat and power

Parameters

A area

GR growth rate

T^{in} designed indoor temperature

U heat transfer cofficient

IU impact of a thermal insulation measure

η efficiency

δ solar irradiance

ε installion area

α design margin

CAP operating capacity

CAP^{min} minimum designed capacity

CAP^{max} maximum designed capacity

γ per unit CO_2 emission

r discount rate

GP gas price

SM maintance cost

SE price of grid electricity

FP feed-in tariff of electricity

DSP retrofitting cost per unit area

SSP supply side equipment cost

CER CO_2 emission reduction

ECR energy consumption reduction

Variables

X energy flow

TS thermal storage

Q heat loss

T^{out} outdoor temperature

RA retrofitted area

NST number of equipments for supply side

COP cofficient of performance for GSHP

ΔT temperature difference

EC energy input

OE energy output

SI number of newly invested and retrofitted equipments

RT equipment replacement parameter

μ part load factor

EM CO_2 emission

CC capital cost

OM operation and maintenance cost

IN income

MOTC minimization of total cost

MOCE minimization of CO_2 emissions

MOEC minimization of energy consumption

Z weight coefficient

References

[1] Wang Z-b, Zhang H-l, Lu X-h, Wang M, Chu Q-q, Wen X-y, Chen F. Lowering carbon footprint of winter wheat by improving management practices in North China Plain. Journal of Cleaner Production. 2016;112, Part 1:149-57.

[2] Cadarso MÁ, Gómez N, López LA, Tobarra MÁ. Calculating tourism's carbon footprint: measuring the impact of investments. Journal of Cleaner Production. 2016;111, Part B:529-37.

[3] Zhao H, Wang Y, Yang D, Zhao X, Li N, Zhou Y. An analysis of genetic diversity in Marphysa sanguinea from different geographic populations using ISSR polymorphisms. Biochemical Systematics and Ecology. 2016;64:65-9.

[4] He C, Chen T, Mao X, Zhou Y. Economic transition, urbanization and population redistribution in China. Habitat International. 2016;51:39-47.

[5] Lam HL, Varbanov PS, Klemeš JJ. Regional renewable energy and resource planning. Applied Energy. 2011;88(2):545-50.

[6] Klemeš JJ, Kravanja Z, Varbanov PS, Lam HL. Advanced multimedia engineering education in energy, process integration and optimisation. Applied Energy. 2013;101:33-40.

[7] Ju L, Tan Z, Li H, Tan Q, Yu X, Song X. Multi-objective operation optimization and evaluation model for CCHP and renewable energy based hybrid energy system driven by distributed energy resources in China. Energy. 2016;111:322-40.

[8] Gustafsson S-I, Karlsson BG. Life-cycle cost minimization considering retrofits in multi-family residences. Energy and Buildings. 1989;14(1):9-17.

[9] Adamo L, Cammarata G, Fichera A, Marletta L. Improvement of a district heating network through thermoeconomic approach. Renewable Energy. 1997;10(2–3):213-6.

[10] Henning D. MODEST—An energy-system optimisation model applicable to local utilities and countries. Energy. 1997;22(12):1135-50.

[11] Li L, Mu H, Li N, Li M. Economic and environmental optimization for distributed energy resource systems coupled with district energy networks. Energy. 2016;109:947-60.

[12] Falke T, Krengel S, Meinerzhagen A-K, Schnettler A. Multi-objective optimization and simulation model for the design of distributed energy systems. Applied Energy. 2016;184:1508-16.

[13] Keirstead J, Samsatli N, Shah N, Weber C. The impact of CHP (combined heat and power) planning restrictions on the efficiency of urban energy systems. Energy. 2012;41(1):93-103.

[14] Jennings M, Fisk D, Shah N. Modelling and optimization of retrofitting residential energy systems at the urban scale. Energy. 2014;64:220-33.

[15] Rolfsman B. Optimal supply and demand investments in municipal energy systems. Energy Conversion and Management. 2004;45(4):595-611.

[16] Giannoulis ED, Haralambopoulos DA. Distributed Generation in an isolated grid:

Methodology of case study for Lesvos - Greece. Applied Energy. 2011;88(7):2530-40.
[17] Capuder T, Mancarella P. Techno-economic and environmental modelling and optimization of flexible distributed multi-generation options. Energy. 2014;71:516-33.
[18] Dong M, He F, Wei H. Energy supply network design optimization for distributed energy systems. Computers & Industrial Engineering. 2012;63(3):546-52.
[19] Bridier L, David M, Lauret P. Optimal design of a storage system coupled with intermittent renewables. Renewable Energy. 2014;67:2-9.
[20] Hong T, Kim D, Koo C, Kim J. Framework for establishing the optimal implementation strategy of a fuel-cell-based combined heat and power system: Focused on multi-family housing complex. Applied Energy. 2014;127:11-24.
[21] Voll P, Lampe M, Wrobel G, Bardow A. Superstructure-free synthesis and optimization of distributed industrial energy supply systems. Energy. 2012;45(1):424-35.
[22] Chen Y, Lu H, Li J, Huang G, He L. Regional planning of new-energy systems within multi-period and multi-option contexts: A case study of Fengtai, Beijing, China. Renewable and Sustainable Energy Reviews. 2016;65:356-72.
[23] Olsthoorn D, Haghighat F, Mirzaei PA. Integration of storage and renewable energy into district heating systems: A review of modelling and optimization. Solar Energy. 2016;136:49-64.
[24] Theo WL, Lim JS, Ho WS, Hashim H, Lee CT. Review of distributed generation (DG) system planning and optimisation techniques: Comparison of numerical and mathematical modelling methods. Renewable and Sustainable Energy Reviews. 2017;67:531-73.
[25] Siddaiah R, Saini RP. A review on planning, configurations, modeling and optimization techniques of hybrid renewable energy systems for off grid applications. Renewable and Sustainable Energy Reviews. 2016;58:376-96.
[26] Gustafsson S-I. Optimisation of insulation measures on existing buildings. Energy and Buildings. 2000;33(1):49-55.
[27] CIBSE. Energy efficiency in building: CIBSE guide F. london, UK: The Chartered Institution of Building Services Engineers. 2012.
[28] Wu X, Olesen BW, Fang L, Zhao J, Wang F. Indoor temperatures for calculating room heat loss and heating capacity of radiant heating systems combined with mechanical ventilation systems. Energy and Buildings. 2016;112:141-8.
[29] Martínez-Lera S, Ballester J, Martínez-Lera J. Analysis and sizing of thermal energy storage in combined heating, cooling and power plants for buildings. Applied Energy. 2013;106:127-42.
[30] Cossu M, Murgia L, Ledda L, Deligios PA, Sirigu A, Chessa F, Pazzona A. Solar radiation distribution inside a greenhouse with south-oriented photovoltaic roofs and effects on crop productivity. Applied Energy. 2014;133:89-100.
[31] Staffell I, Brett D, Brandon N, Hawkes A. A review of domestic heat pumps. Energy &

Environmental Science. 2012;5(11):9291-306.
[32] Li M, Mu H, Li N, Ma B. Optimal design and operation strategy for integrated evaluation of CCHP (combined cooling heating and power) system. Energy. 2016;99:202-20.
[33] Cho H, Luck R, Eksioglu SD, Chamra LM. Cost-optimized real-time operation of CHP systems. Energy and Buildings. 2009;41(4):445-51.
[34] Dhakal S. Urban energy use and carbon emissions from cities in China and policy implications. Energy Policy. 2009;37(11):4208-19.
[35] Weber C, Maréchal F, Favrat D. Design and optimization of district energy systems. In: Valentin P, Paul Şerban A, editors. Computer Aided Chemical Engineering: Elsevier; 2007. p. 1127-32.
[36] Wang H, Yin W, Abdollahi E, Lahdelma R, Jiao W. Modelling and optimization of CHP based district heating system with renewable energy production and energy storage. Applied Energy. 2015;159:401-21.
[37] Wang J, Zhai ZJ, Zhang C, Jing Y. Environmental impact analysis of BCHP system in different climate zones in China. Energy. 2010;35(10):4208-16.

Figure captions:

Fig. 1. Zonal layout of the industrial park, where the green square 1 covers its industrial area and the blue square 2 covers its residential area.

Fig. 2. Daily temperature of Xi'an for different seasons in a year.

Fig. 3. Flow diagram of the urban energy system for the test case.

Fig. 4. Optimal selection and operation of technologies for electricity supply in summer.

Fig. 5. Optimal selection and operation of technologies for heating supply in winter.

Fig. 6 Optimal propotion of retrofit areas of building elements under different scenarios.

Fig.7 Percentage variations in CER and ECR with different selections of technology mix (compared to the reference case).

Fig.8 Interactions between CER and ECR as well as the effect of CER and ECR on the NPV and operating cost of the system (compared to baseline scenario).

Table captions:

Table 1. Initial area (m^2) of building envelopes for each spatial area of the test case.

Table 2. Thermal conductivities of different building elements before and after retrofit.

Table 3. Values of selected parameters [30, 34-37].

Table 4. Optimization results of the test case for different scenarios.

Table 5. Optimization results of three sub-objectives and the multi-objective.

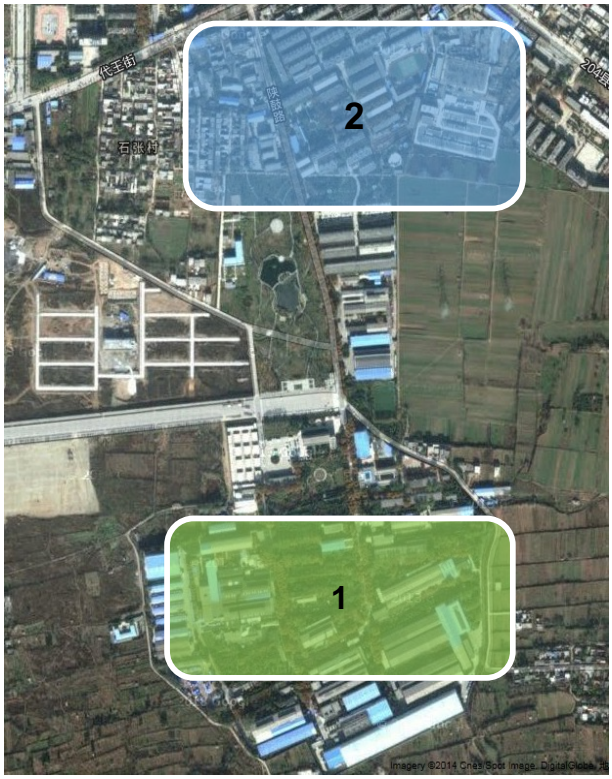


Fig. 1. Zonal layout of the industrial park, where the green square 1 covers its industrial area and the blue square 2 covers its residential area.

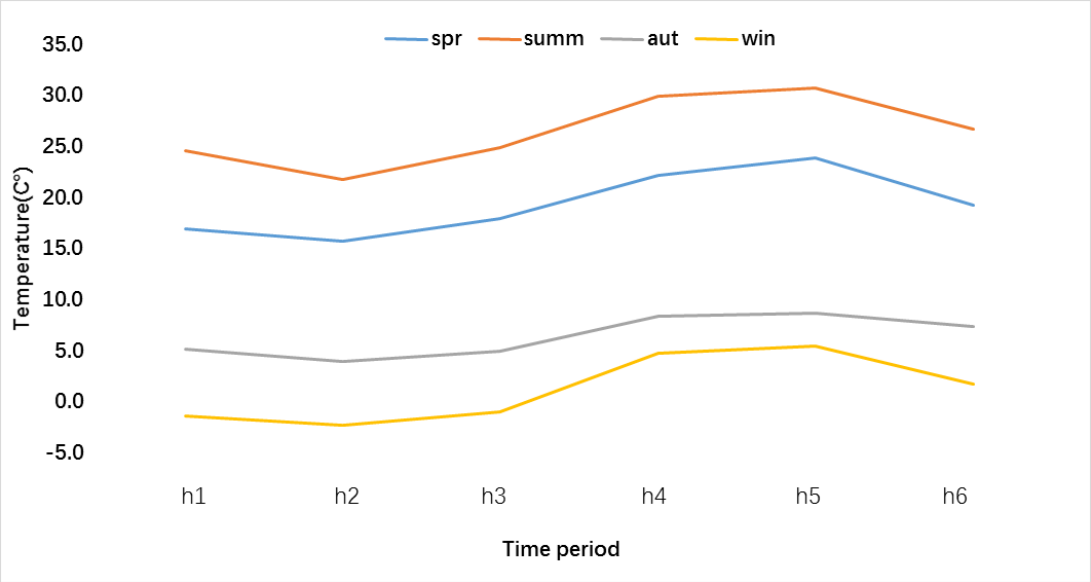


Fig. 2. Daily temperature of Xi'an for different seasons in a year.

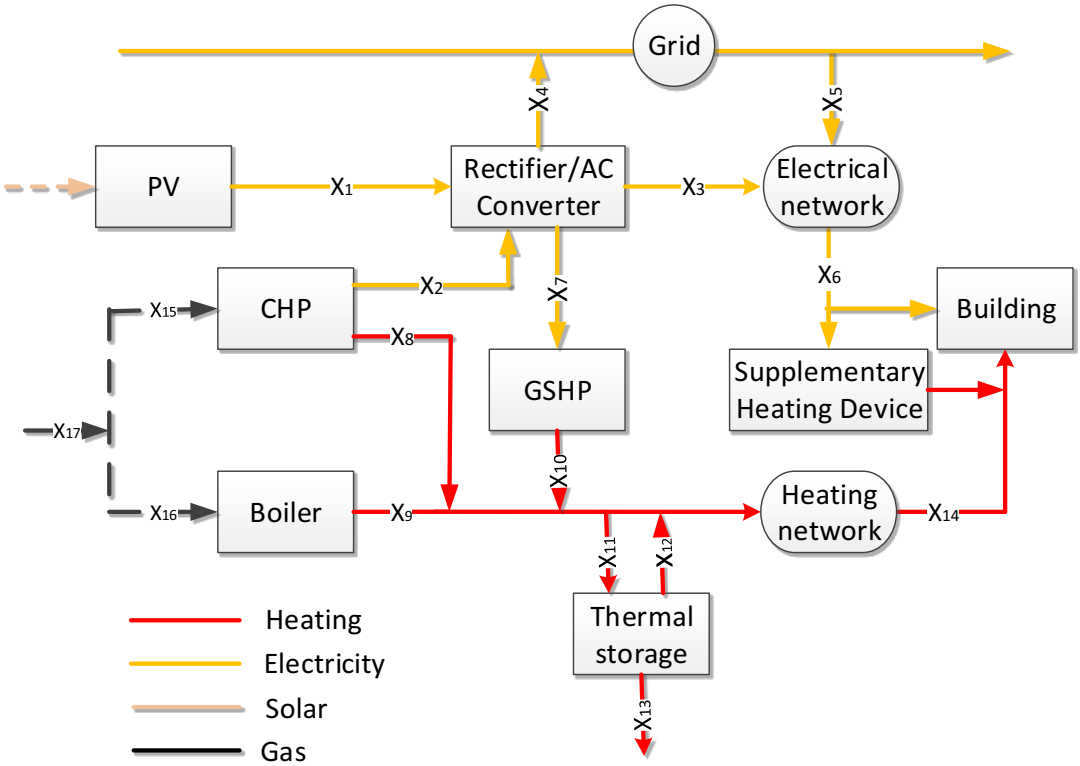


Fig. 3. Flow diagram of the urban energy system for the test case.

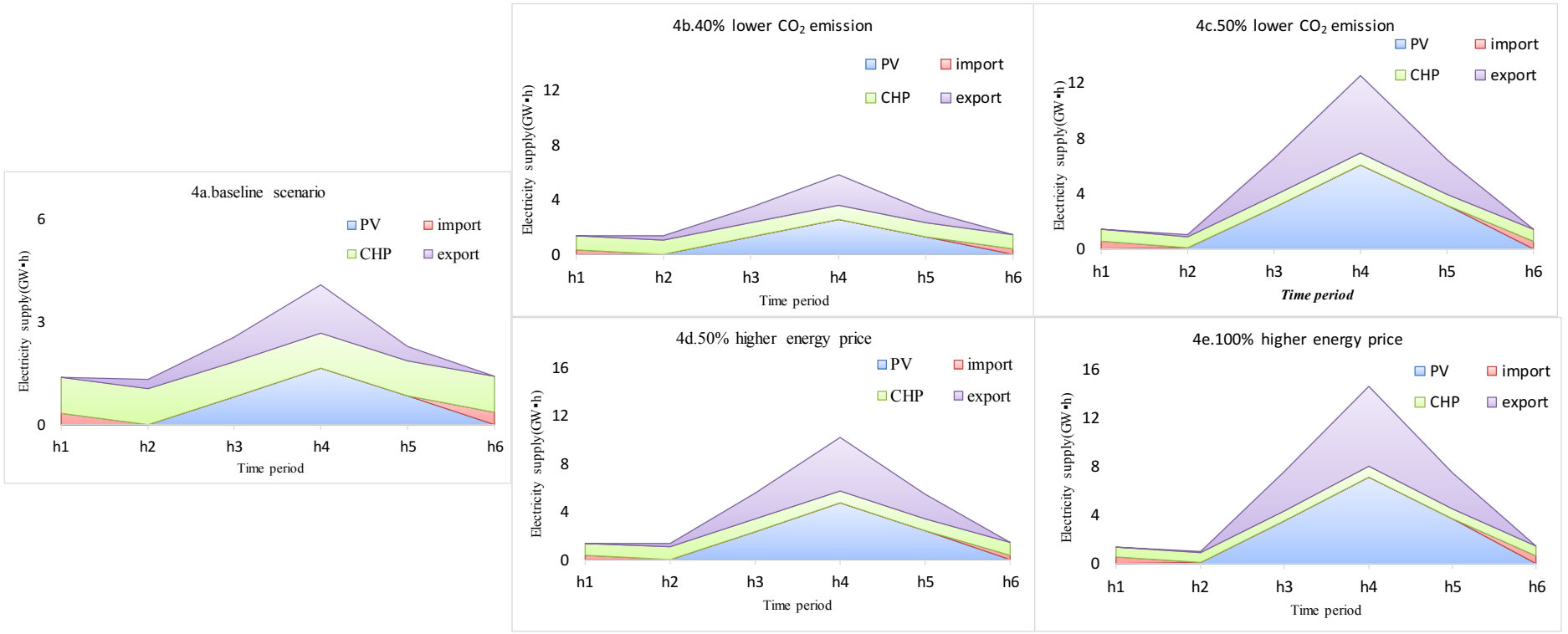


Fig. 4. Optimal selection and operation of technologies for electricity supply in summer.

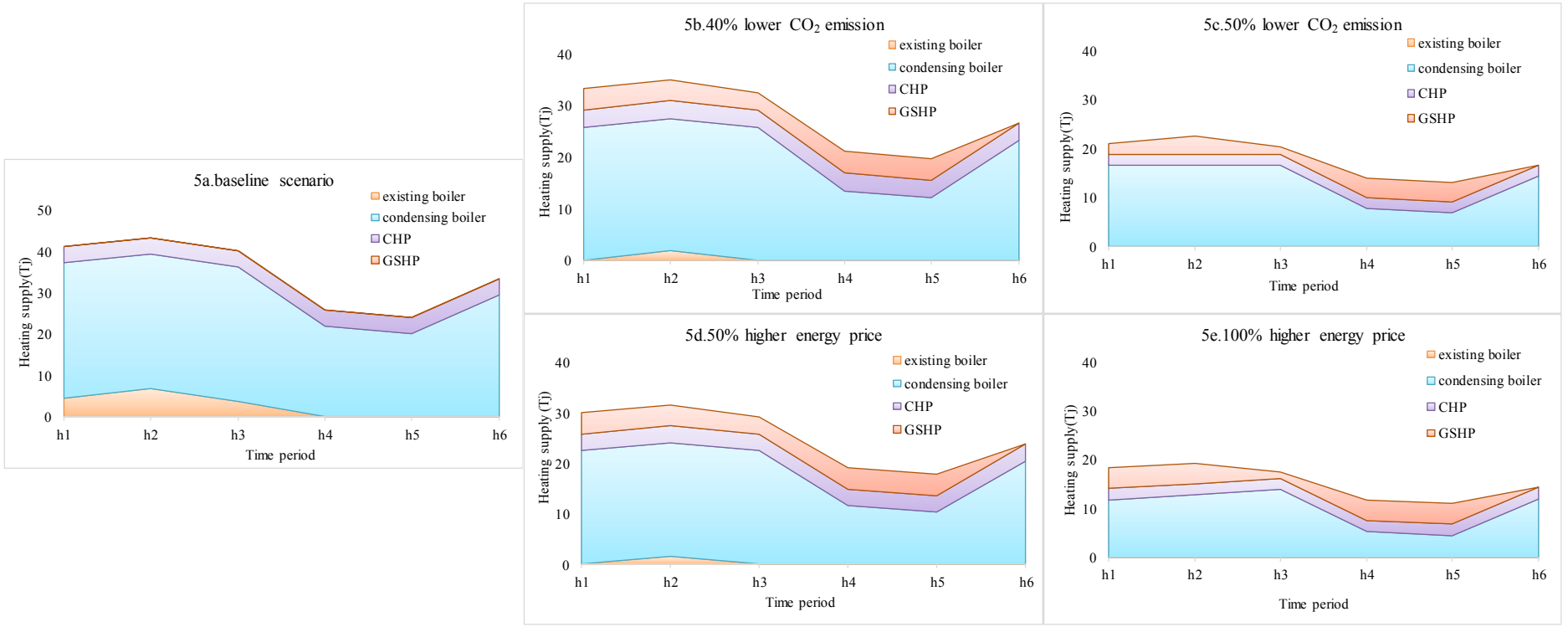


Fig. 5. Optimal selection and operation of technologies for heating supply in winter.

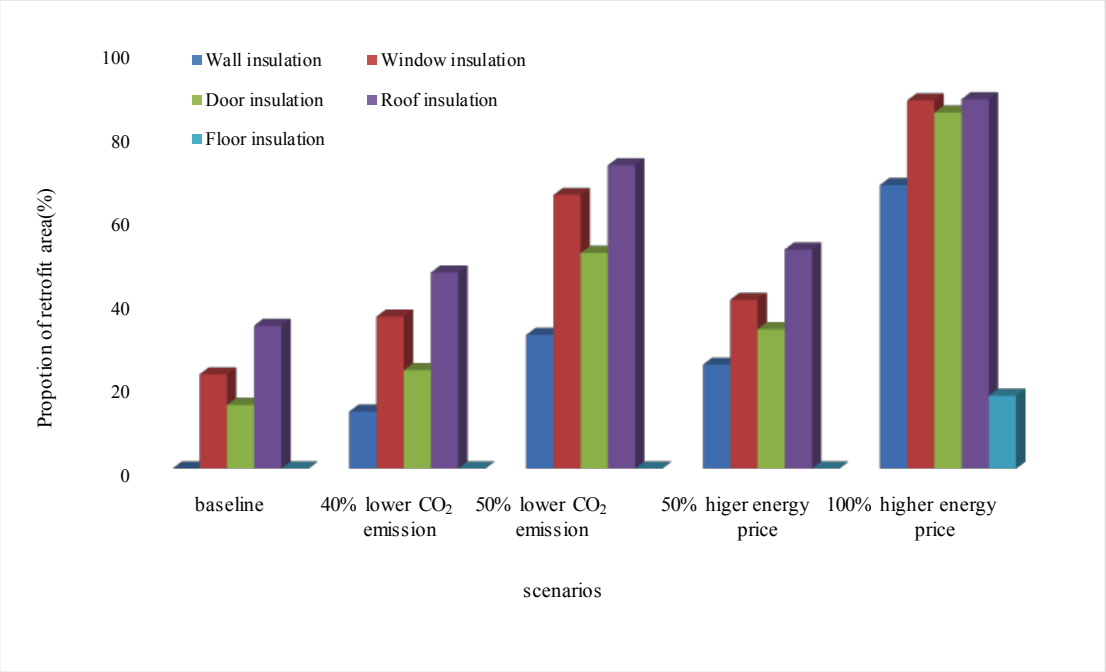


Fig. 6 Optimal propotion of retrofit areas of building elements under different scenarios.

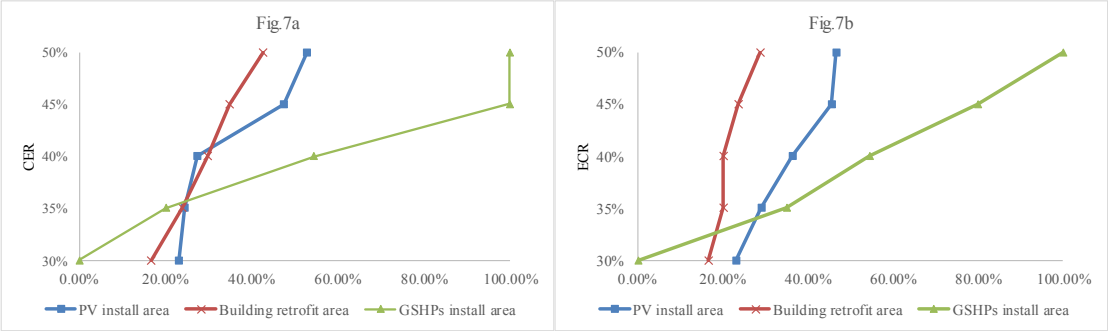


Fig.7 Percentage variations in CER and ECR with different selections of technology mix (compared to the reference case)

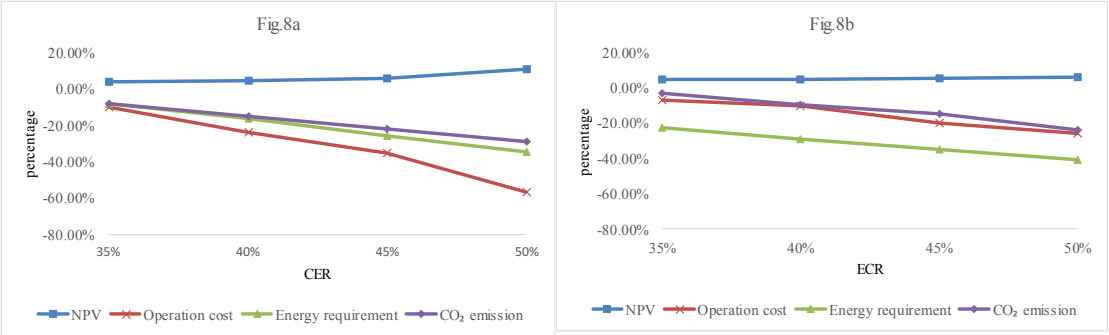


Fig.8 Interactions between CER and ECR as well as the effect of CER and ECR on the NPV and operating cost of the system (compared to baseline scenario)

Spatial area \ Element(m^2)	Exterior wall	Exterior window	Roof	Exterior door	Floor
1	145535	58214	191015	29107	180100
2	32617	9785.1	24462	4892.1	22831

Table 1. Initial area (m^2) of building envelopes for each spatial area of the test case.

Building elements	U before retrofit ($W/m^2 \cdot K$)	U after retrofit ($W/m^2 \cdot K$)	criterion ($W/m^2 \cdot K$)
Exterior wall	1.92	0.6	≦0.6
Exterior window	4.71	2.81	≦3.2
Roof	3.23	0.49	≦0.6
Door	2.03	1.45	-
Floor	0.88	0.44	-

Table 2. Thermal conductivities of different building elements before and after retrofit.

Parameter	Symbol	Value
CO_2 emission per unit generation of grid electricity	γ_{el}	0.977 kg/kW▪h
CO_2 emission per unit consumption of natural gas	γ_{gas}	2.1622 kg/m³
Photovoltaic efficiency	η_{pv}	14.20%
Partload factor	μ	25%~100%
Electrical efficiency of CHP	η_{chp}^{el}	42.30%
Thermal efficiency of CHP	η_{chp}^{th}	42.70%
Electricity efficiency of grid	η_{grid}	35%
Price of CHP	*chp*	5000 RMB/kW
Price of condensing boiler	*boiler*	350 RMB/kW
Price of roof-PV system	*pv*	10000 RMB/kW
Price of ground source heat pump	*gshp*	3500 RMB/kW
Price of thermal storage tank	*TS*	1100 RMB/m^3

Table 3. Values of selected parameters【30,34-37】.

scenarios / results	Reference case	Baseline	Reduce 40% CO_2 emission	Reduce 50% CO_2 emission	50% Higher energy prices	100% Higher energy prices
Wall insulation (%)	-	-	13.6	31.9	24.8	67.7
Window insulation (%)	-	22.5	36.3	65.3	40.3	87.9
Door insulation (%)	-	15.2	23.5	51.5	33.3	85.0
Roof insulation (%)	-	34.1	46.8	72.4	52.3	88.2
Floor insulation (%)	-	0	0	0	0	17.4
Electricity supplied by PVs (%)	-	27.7	36.0	61.2	51.5	66.5
Electricity supplied by CHPs (%)	-	67.2	57.0	32.9	44.1	32.0
Electricity imported from GRID (%)	100.0	5.1	6.8	5.9	4.4	1.5
Total heating requirements (TJ)	443.6	371.5	332.2	262.6	314.1	187.7
Heating supplied by existing boilers (%)	100.0	3.6	0.9	0.0	1.1	0.0
Heating supplied by condensing boilers (%)	-	73.7	62.1	52.3	59.8	48.2
Heating supplied by GSHPs (%)	-	0.0	13.7	17.7	14.5	22.2
Heating supplied by CHPs (%)	-	22.7	24.2	30.0	25.7	29.6
Electricity sold back to GRID (GW·h)	-	9.0	12.3	30.2	24.7	35.1
NPV (million RMB)	-	277.8	292.2	308.1	406.7	515.8

Table 4. Optimization results of the test case for different scenarios.

	NPV(million RMB)	CO_2 emissions(kt)	ER(TJ)	weight(%)
MOTC	277.80	346.00	5478.62	25.41
MOCE	388.75	264.25	4054.71	39.48
MOEC	349.13	279.27	3565.24	35.11
Maximum	388.75	346.00	5478.62	-
Minimum	277.80	264.25	3565.24	-
IE	337.14	266.27	4008.74	-

Table.5 Optimization results of three sub-objectives and the multi-objective (MOTC, MOCE, MOEC represent the minimization of total cost, CO2 emissions and energy consumption, respectively).